

Photo-crosslinked alginate hydrogels support enhanced matrix accumulation by nucleus pulposus cells *in vivo*

A. I. Chou^{†a}, S. O. Akintoye^{‡b} and S. B. Nicoll^{†§*}

[†] Department of Bioengineering, University of Pennsylvania, 240 Skirkanich Hall, 210 South 33rd Street, Philadelphia, PA 19104-6321, United States

[‡] Department of Oral Medicine, University of Pennsylvania, 209 Robert Schattner Center, 240 South 40th Street, Philadelphia, PA 19104, United States

[§] Department of Orthopaedic Surgery, University of Pennsylvania, Philadelphia, PA 19104, United States

Summary

Objective: Intervertebral disc (IVD) degeneration is a major health concern in the United States. Replacement of the nucleus pulposus (NP) with injectable biomaterials represents a potential treatment strategy for IVD degeneration. The objective of this study was to characterize the extracellular matrix (ECM) assembly and functional properties of NP cell-encapsulated, photo-crosslinked alginate hydrogels in comparison to ionically crosslinked alginate constructs.

Methods: Methacrylated alginate was synthesized by esterification of hydroxyl groups with methacrylic anhydride. Bovine NP cells were encapsulated in alginate hydrogels by ionic crosslinking using CaCl_2 or through photo-crosslinking upon exposure to long-wave UV light in the presence of a photoinitiator. The hydrogels were evaluated *in vitro* by gross and histological analysis and *in vivo* using a murine subcutaneous pouch model. *In vivo* samples were analyzed for gene expression, ECM localization and accumulation, and equilibrium mechanical properties.

Results: Ionically crosslinked hydrogels exhibited inferior proteoglycan accumulation *in vitro* and were unable to maintain structural integrity *in vivo*. In further studies, photo-crosslinked alginate hydrogels were implanted for up to 8 weeks to examine NP tissue formation. Photo-crosslinked hydrogels displayed temporal increases in gene expression and assembly of type II collagen and proteoglycans. Additionally, hydrogels remained intact over the duration of the study and the equilibrium Young's modulus increased from 1.24 ± 0.09 kPa to 4.31 ± 1.39 kPa, indicating the formation of functional matrix with properties comparable to those of the native NP.

Conclusions: These findings support the use of photo-crosslinked alginate hydrogels as biomaterial scaffolds for NP replacement.

© 2009 Osteoarthritis Research Society International. Published by Elsevier Ltd. All rights reserved.

Key words: Nucleus pulposus, Alginate, Hydrogel, Proteoglycan, Type II collagen, Young's modulus.

Introduction

The intervertebral disc (IVD) is a fibro-cartilaginous tissue that confers flexibility to the spine by permitting limited bending and twisting movements between vertebral bodies. The disc is a heterogeneous structure divided into three anatomical regions: the outer and inner annulus fibrosus (AF) and the nucleus pulposus (NP). The outer AF is rich in type I collagen organized into concentric lamellae and allows the disc to resist tensile loads^{1–3}. The NP is composed primarily of negatively charged proteoglycans (i.e., aggrecan) and type II collagen that permit the disc to resist compressive loads by generation of osmotic swelling pressure^{2–4}. The inner AF is considered a transition zone between the highly organized collagenous structure of the outer annulus and the less organized and highly hydrated NP. The loss of

proteoglycans from the NP that occurs with disc degeneration as a result of age or excessive trauma gives rise to a variety of health problems, ranging from lower back pain to paraplegia^{5–7}. Existing surgical interventions do not adequately restore disc function and often reduce joint mobility⁸. Therefore, engineered constructs comprised of natural or synthetic materials have been explored as potential replacements for the disc.

Many naturally derived materials have been examined for IVD tissue reconstruction, including but not limited to, collagen-derived scaffolds (i.e., atelocollagen, and types I and II collagen sponges), chitosan hydrogels, hyaluronic acid hydrogels, and alginate hydrogels^{9–34}. Most studies approximate the NP with a hydrogel-like scaffold that maintains the cells in a chondrocyte-like morphology. In particular, ionically crosslinked alginate hydrogels have been widely characterized and investigated for multiple tissue engineering applications. It is considered a routine method for *in vitro* culture of NP cells^{14–25}. Alginate is a naturally derived polysaccharide extracted from brown algae, which possesses negatively charged carboxyl groups at physiologic pH. In the presence of divalent cations, the alginate is crosslinked to produce a three-dimensional construct. Previous studies have focused on characterizing gene expression and accumulation of extracellular matrix (ECM) macromolecules,

^aTel: 1-215-898-1958; Fax: 1-215-573-2071.

^bTel: 1-215-898-9932; Fax: 1-215-573-7853.

*Address correspondence and reprint requests to: Steven B. Nicoll, Department of Bioengineering, University of Pennsylvania, 240 Skirkanich Hall, 210 South 33rd Street, Philadelphia, PA 19104-6321, United States. Tel: 1-215-573-2626; Fax: 1-215-573-2071; E-mail: aic@seas.upenn.edu, akintoye@dental.upenn.edu, nicoll@seas.upenn.edu

Received 4 July 2008; revision accepted 16 April 2009.

such as type II collagen and proteoglycans. Few, however, have focused on the functional properties of accumulated matrix proteins. Baer *et al.* were first to study functional matrix production in cell-encapsulated ionically crosslinked alginate hydrogels³⁵. They found that cells were not capable of producing a functional matrix over 16 weeks *in vitro*. The authors hypothesized that diffusion and cellular uptake of the cationic crosslinkers were responsible for the adverse mechanical properties. Later, Mizuno *et al.* fabricated a composite IVD structure using a poly(glycolic acid)/poly(L-lactic acid) fiber mesh to approximate the AF and ionically crosslinked alginate to mimic the NP, and implanted the composite scaffold in the subcutaneous dorsa of athymic mice^{27,29}. After 16 weeks post-implantation, the construct resembled native tissue and exhibited increased compressive properties similar to that of native tissue²⁷. These results suggest that further investigation of alginate hydrogels may be required to determine whether the biomaterial is appropriate for IVD tissue regeneration.

Recent work in the synthesis of *in situ* photo-crosslinkable polymers may provide an alternative method for producing alginate hydrogels for NP replacement^{36–42}. In this system, polymers are modified with functional groups (i.e., methacrylates) that undergo free radical polymerization in the presence of a photoinitiator and upon exposure to UV light. This polymerization reaction induces a fluid–solid phase transformation under physiologic conditions and is ideal for encapsulation of cells *in situ*^{43–45}. Elisseff *et al.* used this methodology to successfully encapsulate chondrocytes in poly(ethylene oxide)-based hydrogels for potential use in cartilage repair applications⁴². The technique was modified by Bryant *et al.* to incorporate hydrolytically degradable lactic acid units into photo-crosslinked poly(ethylene glycol)-based hydrogels to enhance the spatial distribution of ECM components in these otherwise inert polymers³⁶. Methacrylated alginate and hyaluronic acid, which are more analogous to the negatively charged mucopolysaccharides in cartilaginous tissues (in comparison to the synthetic ethylene glycol derivatives), have also been studied as platforms for tissue engineering replacement strategies^{43,44,46,47}. However, photo-crosslinked alginate has not been used previously for cell encapsulation or for NP repair. Therefore, the objective of this study was to characterize photo-crosslinked alginate hydrogels for NP tissue formation *in vivo*, specifically focusing on the ability of these materials to support functional ECM assembly by encapsulated NP cells. In this study, modified alginate hydrogels were ionically and photo-crosslinked, and cultured *in vitro* (4 weeks) as well as evaluated *in vivo* using a murine subcutaneous pouch model (over 8 weeks). Hydrogels were analyzed for gene expression, ECM accumulation and distribution, and mechanical properties. We hypothesized that photo-crosslinked alginate hydrogels would exhibit increased structural integrity, ECM accumulation, and mechanical properties compared to ionically crosslinked alginate constructs.

Methods

PRIMARY CELL ISOLATION

Adult bovine tails were obtained from a local abattoir and caudal disc tissue excised from levels C2 to C4 in a sterile environment. The NP was separated through gross visual inspection. All tissues were maintained in Dulbecco's Modified Essential Medium (DMEM) with 20% Fetal Bovine Serum (FBS, Hyclone, Logan, UT), 2.5 µg/mL fungizone reagent, 100 U/ml penicillin, 100 µg/ml streptomycin, and 0.075% NaHCO₃ (primary media) for 1 day at 37°C in a humidified atmosphere with 5% CO₂ to confirm that no

contamination occurred during the harvesting process. Tissue was diced and cells were released through collagenase digestion as previously described⁴⁸. Released cells were designated passage 0 and serially passaged twice according to previous protocols^{15,49}.

MACROMER SYNTHESIS

Methacrylated alginate (MA-LVALG) was synthesized through esterification of hydroxyl groups based on protocols previously described^{43,44}. Briefly, a 1% solution of low viscosity alginate (LVALG, Sigma, St. Louis, MO) was prepared in deionized water and adjusted to pH 8 using 5 N NaOH. Methacrylic anhydride (Sigma, St. Louis, MO) at 20-fold excess was added to the alginate solution slowly at 4°C and the pH was periodically adjusted to 8 using 5 N NaOH (approximately 15 times over the course of the 24-h reaction). The solution was allowed to react for 24 h at 4°C. The modified alginate was purified *via* dialysis against sterile water (Spectra/Por 1, MW 5–8 kDa, Rancho Dominguez, CA) for 48 h to remove excess methacrylic anhydride and the final product was recovered by lyophilization. The degree of substitution was confirmed using ¹H-NMR analysis (DMX 360) with D₂O as the solvent. The relative integrations of the methacrylate proton peaks (methylene, δ = 6.0 and 5.6 ppm and the methyl peak, δ = 1.8 ppm) to carbohydrate protons were used to determine molar percent of methacrylation. A 3.5% modified MA-LVALG was synthesized and used for all subsequent studies.

ALGinate HYDROGEL PREPARATIONS

All ionically and photo-crosslinked cell-encapsulated alginate constructs were prepared with 3.5% modified MA-LVALG at 2 w/v% based on our previous studies⁵⁰. Prior to dissolution, lyophilized MA-LVALG was sterilized by exposure to germicidal UV light for 30 min. MA-LVALG was dissolved in a 0.05% filter-sterilized solution of the photoinitiator 2-methyl-1-[4-(hydroxyethoxy)phenyl]-2-methyl-1-propanone (Irgacure 2959, I2959, Ciba Specialty Chemicals, Basel, Switzerland) in calcium and magnesium-free Dulbecco's Phosphate Buffered Saline (DPBS) at 2.2 w/v%. An NP cell suspension in DPBS (10 × 10⁶ cells/mL final MA-LVALG) was added and homogeneously mixed with MA-LVALG and cast at a final concentration of 2 w/v%. For photo-crosslinked MA-LVALG hydrogels, a cell-polymer solution was cast in a custom-made glass casting device and exposed to long-wave UV light (EIKO, Shawnee, KS, peak 368 nm, 1.2 W) for 10 min to produce 2-mm thick, 8-mm diameter hydrogels. For ionically crosslinked MA-LVALG hydrogels, a cell-polymer solution was cast into a custom-designed gel casting device between two sheets of filter paper soaked in 102 mM CaCl₂. After 10 min, the top of the cast was removed and submerged in a 102 mM CaCl₂ bath for an additional 10 min to produce 2-mm thick, 8-mm diameter hydrogels. Acellular hydrogel controls were also prepared for all groups.

PRELIMINARY *IN VITRO* AND *IN VIVO* CROSSLINKING STUDY

Using MA-LVALG, ionically and photo-crosslinked alginate hydrogels were prepared as described above. Ionically and photo-crosslinked samples were incubated *in vitro* with 3 mL of growth medium (DMEM with 10% FBS, 100 U/ml penicillin, 100 µg/ml streptomycin, and 0.075% NaHCO₃) and supplemented with vitamin C (50 µg/mL) at day 1 and replaced every 2–3 days. All *in vitro* hydrogels were maintained at 37°C in a humidified atmosphere with 5% CO₂. Ionically and photo-crosslinked hydrogels were also implanted subcutaneously in a murine pouch model as described below. Samples were isolated at 4 weeks for gross inspection and immunohistochemical analysis.

IN VIVO MURINE SUBCUTANEOUS POUCH MODEL

Cell-seeded and acellular hydrogel constructs were prepared as described above and implanted subcutaneously in immunocompromised 6–8-week-old female beige mice (Strain: NIH-III-nu, Charles River Laboratories, Wilmington, MA) in accordance with University of Pennsylvania guidelines for the use of vertebrate animals for research (animal protocol # 800209). Surgery was performed aseptically under anesthesia induced by injection of 140 mg/kg body weight of ketamine (Fort Dodge, Animal Health, Fort Dodge, IA), 7 mg/kg body weight xylazine (Phoenix Pharmaceuticals, St Joseph, MO) and 1 mg/kg body weight acepromazine (Burns Veterinary Supply, Farmers Branch, TX). A mid-longitudinal sagittal skin incision on the dorsum of each mouse was expanded by blunt dissection to create separate subcutaneous pockets for a set of four individual hydrogel implants. Each mouse received the four implants to reduce variability among samples. The skin incision was closed with absorbable 3–0 Vicryl® sutures (Ethicon Inc., Somerville, NJ). Implants were harvested at 4 (ionically and photo-crosslinked hydrogels) and 8 (photo-crosslinked hydrogels only) weeks. The animals were euthanized by CO₂ asphyxiation in accordance with the guidelines established by the American Veterinary Medical Association Panel on Euthanasia.

GENE EXPRESSION

At 4 and 8 weeks post-implantation, RNA was isolated from freshly harvested *in vivo* constructs to evaluate gene expression⁴⁸. Cells were released from the photo-crosslinked alginate hydrogels by addition of 20 mg/mL of alginate lyase (Sigma, St. Louis, MO) in DPBS (1 mL per hydrogel), and incubated on an orbital shaker at 37°C until the alginate was fully dissolved (approximately 30 min). Cells were pelleted by centrifugation (2000 rcf, 5 min) and RNA was extracted and purified using the RNeasy kit (Qiagen, Valencia, CA). Purity and concentration of all RNA were assessed spectrophotometrically. Reverse transcription (RT) was performed using the Superscript First-Strand Synthesis System for RT-polymerase chain reaction (PCR) (Invitrogen) and real-time PCR was conducted using the SYBR Green Master Mix Kit (Applied Biosystems, Foster City, CA) and an Applied Biosystems 7300 real-time PCR system. Primers for collagen type I, collagen type II, aggrecan, and glyceraldehyde-3-phosphate dehydrogenase (GAPDH) were as published⁵¹. Types I and II collagen and aggrecan gene expression were normalized to GAPDH expression and fold differences were calculated using the $\Delta\Delta C_t$ method.

COLLAGEN QUANTIFICATION

Protein expression of type II collagen was quantified on freshly isolated samples using an indirect enzyme-linked immunosorbent assay (ELISA) as previously described^{48,52}. Briefly, cells encapsulated in alginate hydrogels were released as for RNA isolation and stored in 100–200 μ L of 0.05 N acetic acid at -20°C . To extract proteins, all samples were removed from acetic acid and treated with 3 M guanidine HCl (GuHCl) and 2 mg/ml pepsin. Digests were plated in a 96-well Nunc Maxisorp plate for collagen protein quantification. Antibodies to type II collagen (1:4000) (Rabbit anti-bovine type II collagen polyclonal antibody, Chemicon, Temecula, CA) were used along with a peroxidase-based detection system employing a biotinylated secondary antibody (goat anti-rabbit IgG (H + L), Vector Labs, Burlingame, CA) and a streptavidin-horseradish peroxidase enzyme conjugate (R&D Systems, Minneapolis, MN). Total reacted substrate was spectrophotometrically analyzed at 450 nm using a Bio-Tek Synergy-HT microplate reader (Winooski, Vermont) and total collagen was determined from standard curves of bovine type II collagen (isolated from bovine nasal cartilage, Rockland, Gilbertsville, PA).

SULFATED GLYCOSAMINOGLYCAN (GAG) QUANTIFICATION

Production of sulfated GAGs was quantified on freshly harvested samples using the 1,9-dimethylmethylene blue (DMMB) dye-binding assay⁵³. Protein extracts (Pepsin and GuHCl digests) were allowed to react with DMMB at pH 1.5 (Sigma–Aldrich, St. Louis, MO) and spectrophotometrically analyzed at 595 nm using a Bio-Tek Synergy-HT microplate reader (Winooski, Vermont)⁵⁴. Total GAG was determined from standard curves of chondroitin-6-sulfate C isolated from shark cartilage (Sigma, St. Louis, MO).

MECHANICAL TESTING

Unconfined compression testing was conducted on excised *in vivo* hydrogels at 4 and 8 weeks post-implantation to evaluate the equilibrium Young's modulus. Prior to testing, stereomicrographs were captured using a Zeiss

Stemi 2000-C stereomicroscope and analyzed for hydrogel surface area using Scion image software. The mechanical testing device is based on a similar set-up described by Soltz and Ateshian⁵⁵. Samples were compressed between two impermeable glass platens in a DPBS bath. A protease inhibitor cocktail (10 mM *N*-ethylmaleimide, 1 mM phenyl-methyl-sulfonyl fluoride, 5 mM benzamide) was added to the DPBS bath to prevent matrix degradation over the course of the test⁵⁵. The unconfined compression testing protocol consisted of a creep test followed by a multi-ramp stress-relaxation test⁵⁰. For the creep test, a 1-g tare load was applied at a 10 $\mu\text{m/s}$ ramp velocity for 2100 s, which corresponded to the time when equilibrium was reached (equilibrium criteria: $<10 \mu\text{m}$ change in 10 min). The multi-ramp stress-relaxation test consisted of three 5% strain ramps, each followed by a 2000 s relaxation period (equilibrium criteria for stress-relaxation: $<0.5 \text{ g}$ change in 10 min). Equilibrium stress was calculated at each ramp using surface area data and plotted against the applied strain. From this equilibrium stress vs strain curve, an equilibrium Young's modulus was determined and reported for each sample. After mechanical testing, hydrogels were fixed in acid formalin for 30 min at 4°C for immunohistochemical analysis.

IMMUNOHISTOCHEMISTRY

Fixed samples were paraffin-embedded, sectioned using a Lieca microtome (Model 2030, Nussloch, Germany), and processed for immunohistochemistry to visualize ECM deposition. For collagen immunohistochemistry, samples were pre-treated with hyaluronidase for 30 min at 37°C and 0.5 N acetic acid for 2 h at 4°C. Samples for chondroitin sulfate proteoglycan immunohistochemistry were only treated with 0.5 N acetic acid for 2 h at 4°C. Antibodies to type II collagen (1:40) (Polyclonal Rabbit anti-bovine type II collagen polyclonal antibody, Chemicon, Temecula, CA) and chondroitin sulfate proteoglycan (1:100) (Sigma, St. Louis, MO) were applied. A peroxidase-based detection system (Vectastain Elite ABC, Vector Labs, Burlingame, CA) and 3,3'-diaminobenzidine as the substrate chromagen were used to detect protein localization. Non-immune controls were included without primary antibody. Stained samples were viewed with a Zeiss Axioskop 40 optical microscope and images were captured using AxioVision software.

STATISTICAL ANALYSIS

Data are presented as the mean \pm standard deviation ($n = 4$). A one-way ANOVA was used to determine the effect of time on gene expression, ECM accumulation (normalized type II collagen and GAG content) and the equilibrium Young's modulus. Pairwise comparisons were made using a Tukey post-hoc test and significance was set at $P < 0.05$. Statistical analyses were performed using JMP software (SAS Institute, Cary, NC).

Results

PRELIMINARY ANALYSIS OF IONICALLY AND PHOTO-CROSS-LINKED ALGINATE HYDROGELS *IN VITRO* AND *IN VIVO*

NP cells were encapsulated in ionically and photo-cross-linked methacrylated alginate and cultured *in vitro* as well as evaluated *in vivo* using a murine subcutaneous pouch

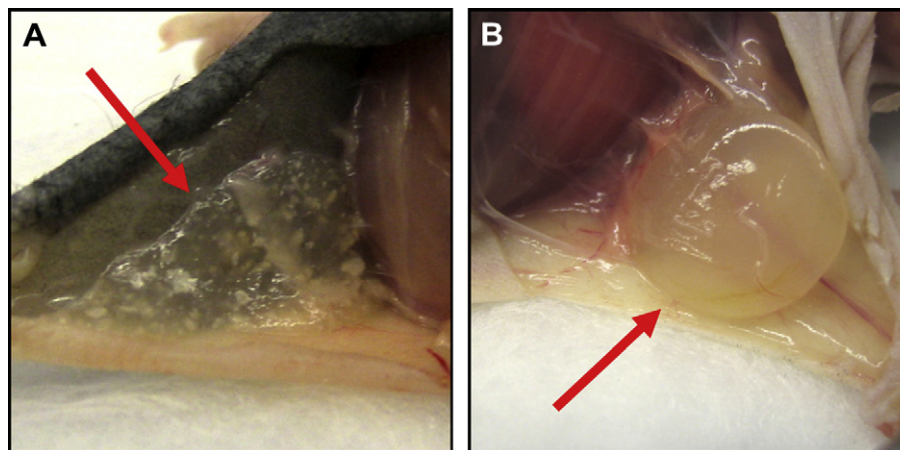


Fig. 1. Methacrylated alginate hydrogels after 4 weeks *in vivo*. Ionically (A) and photo-crosslinked (B) hydrogels. Arrows indicate location of the hydrogel.

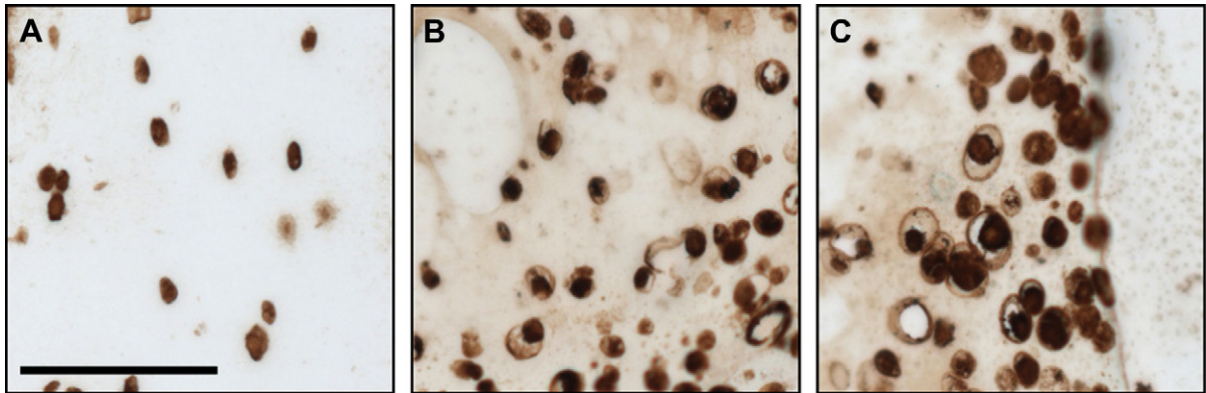


Fig. 2. Chondroitin sulfate proteoglycan immunohistochemistry of ionically and photo-crosslinked alginate hydrogels after 4 weeks of *in vitro* and *in vivo* culture. (A) Ionically crosslinked alginate hydrogel cultured *in vitro*, (B) photo-crosslinked alginate hydrogel cultured *in vitro*, and (C) photo-crosslinked alginate hydrogel *in vivo*. Scale bar = 100 μ m.

model. At 4 weeks *in vitro*, NP cells remained viable in all cultures, with photo-crosslinked hydrogels exhibiting greater viability than ionic alginate hydrogels (data not shown). After 4 weeks *in vivo*, all hydrogels were encapsulated in a thin fibrous capsule consistent with a mild foreign body response. Nevertheless, ionically crosslinked alginate hydrogels had undergone severe dissolution by that time and were unable to be processed for immunohistochemistry [Fig. 1(A)]. Photo-crosslinked hydrogels remained intact and displayed no apparent changes in structural integrity and shape [Fig. 1(B)]. NP cells maintained a rounded morphology in all intact hydrogels (Fig. 2), however, immunohistochemistry revealed more extensive ECM accumulation in photo-crosslinked hydrogels in comparison to ionic alginate hydrogels [Fig. 2(A vs B and C)]. Furthermore, photo-crosslinked hydrogel constructs produced greater amounts of type II collagen (data not shown) and chondroitin sulfate proteoglycan [Fig. 2(B vs C)] *in vivo* compared to those cultured *in vitro*. Based on these initial results, photo-crosslinked alginate hydrogels were evaluated in the murine subcutaneous pouch model in all subsequent studies.

GENE EXPRESSION

Gene expression at 4 and 8 weeks revealed that photo-crosslinked alginate hydrogels support expression of characteristic ECM macromolecules by encapsulated NP cells.

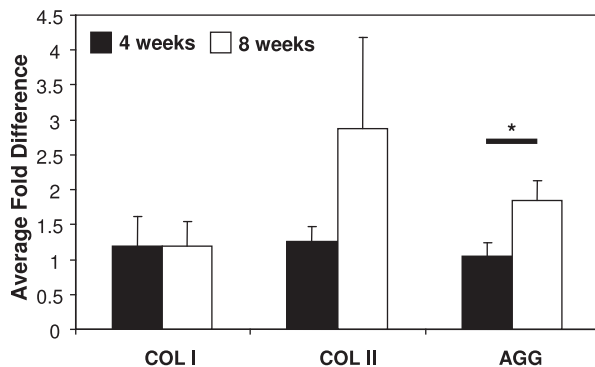


Fig. 3. Quantitative gene expression of types I (COL I) and II (COL II) collagen and aggrecan (AGG) normalized to GAPDH expression at 4 and 8 weeks post-implantation. * denotes a significant difference ($P < 0.05$) between 4 and 8 weeks.

Both type II collagen and aggrecan expression increased while type I collagen expression remained unchanged over time (Fig. 3). However, only aggrecan displayed a significant increase in gene expression (Fig. 3). The RNA yields from acellular controls were not sufficient for quantitative analysis.

BIOCHEMISTRY

Production of type II collagen and sulfated GAGs was quantified for photo-crosslinked hydrogels over the 8-week *in vivo* period. At 8 weeks, cell-seeded constructs contained $0.15 \pm 0.03 \times 10^{-3} \mu\text{g}$ COL II/mg wet weight and $6.3 \pm 2.5 \times 10^{-3} \mu\text{g}$ GAG/mg wet weight. Similar to the gene expression results, greater amounts of both type II collagen and sulfated GAGs were detected at 8 weeks compared to the 4-week time point; however, only sulfated

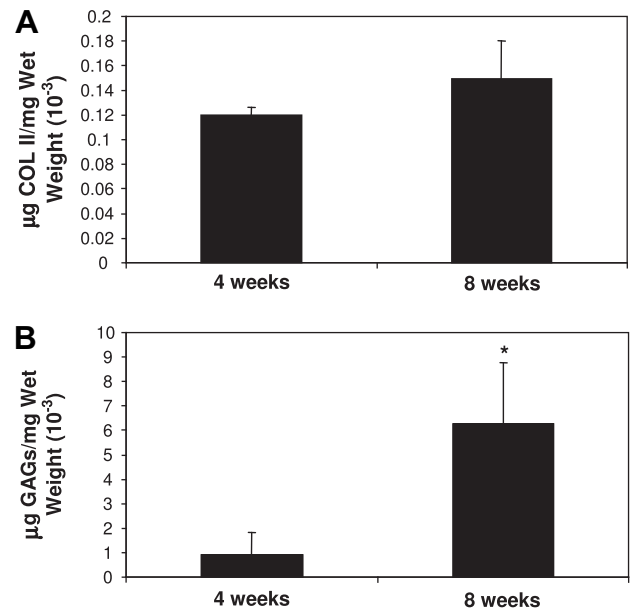


Fig. 4. Total type II collagen (A) and sulfated GAG (B) accumulation normalized to the wet weight of the hydrogels at 4 and 8 weeks post-implantation. * denotes a significant difference between 4 and 8 weeks.

GAGs exhibited a significant increase in accumulation [Fig. 4(A, B)]. Acellular controls did not produce measurable amounts of sulfated GAGs or type II collagen.

IMMUNOHISTOCHEMISTRY

ECM macromolecules secreted by encapsulated NP cells were distributed pericellularly as shown by the immunohistochemical staining of type II collagen and chondroitin sulfate proteoglycan. At 4 weeks, there was relatively little expression of type II collagen in comparison to chondroitin sulfate proteoglycan [Fig. 5(A, B)]. However, by 8 weeks post-implantation, there was an increase in the number of cells producing these characteristic ECM components [Fig. 5(C, D)]. Acellular controls were transparent with no cellular infiltration or detectable matrix accumulation, although remnants of the thin fibrous capsule that enveloped the samples were present on the periphery of the gels (not shown).

MECHANICAL PROPERTIES

The equilibrium Young's modulus of cell-seeded photo-crosslinked constructs reached 4.31 ± 1.39 kPa by 8 weeks

in vivo. At both 4 and 8 weeks post-implantation, the mechanical properties of the photo-crosslinked hydrogels were significantly increased compared to pre-implanted hydrogels [Fig. 6(A)], but there was no significant difference between 4-week and 8-week constructs. Stereomicrographs confirmed an increase in opacity of hydrogels over time [Fig. 6(B–D)]. The equilibrium Young's modulus of acellular controls (2.34 ± 0.33 kPa) was significantly lower than cell-seeded hydrogels at 4 and 8 weeks.

Discussion

In this study, NP cells were encapsulated in ionically and photo-crosslinked alginate hydrogels and evaluated *in vitro* and *in vivo*. Ionically crosslinked alginate hydrogels were unable to maintain their structural integrity and displayed decreased cell numbers and characteristic ECM accumulation compared to photo-crosslinked hydrogels. In further studies, NP cell-encapsulated, photo-crosslinked alginate hydrogels exhibited a significant increase in aggrecan gene expression and total sulfated proteoglycan accumulation over time. Furthermore, the equilibrium Young's modulus demonstrated significant increases, indicating the production of a mechanically functional ECM. These findings support the use of

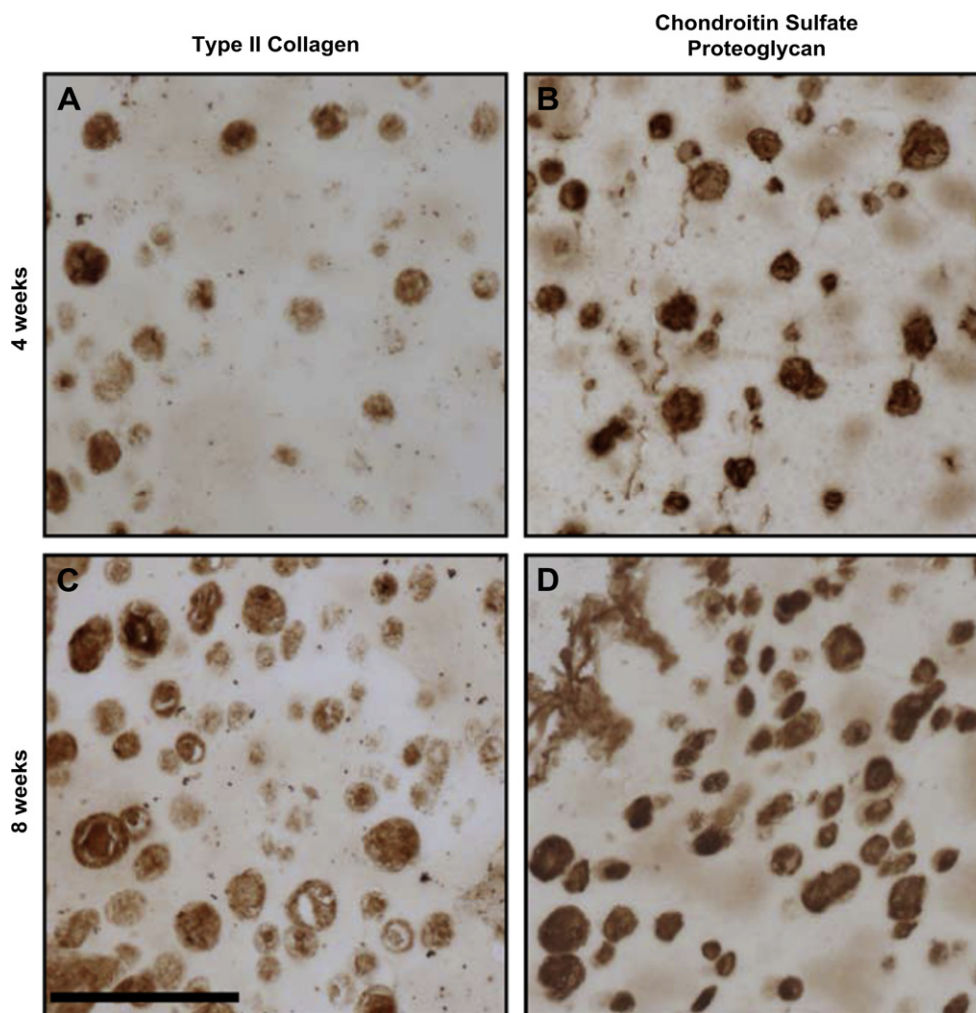


Fig. 5. Immunohistochemistry of type II collagen (A, C) and chondroitin sulfate proteoglycan (B, D) ECM elaboration of photo-crosslinked alginate hydrogels at 4 (A, B) and 8 (C, D) weeks post-implantation. Scale bar = 100 μ m.

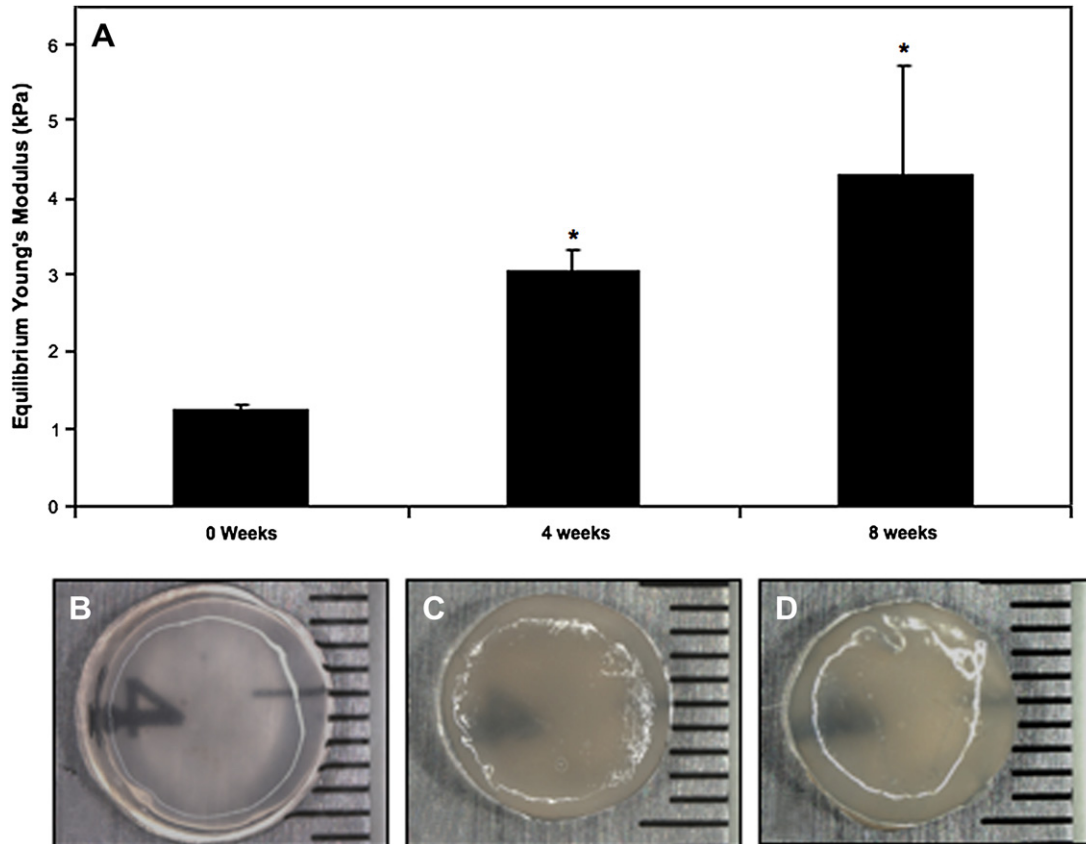


Fig. 6. Equilibrium Young's Modulus of photo-crosslinked alginate hydrogels cultured *in vivo* (A). Representative stereomicrographs of NP cell-encapsulated, photo-crosslinked alginate hydrogels pre-implantation (B), at 4 weeks post-implantation (C), and at 8 weeks post-implantation (D). Scale in mm. * denotes a significant difference ($P < 0.05$) between cell-encapsulated and day 0 controls.

photo-crosslinked alginate hydrogels for functional matrix accumulation by encapsulated NP cells.

Ionically crosslinked hydrogels experienced significant dissolution *in vivo* compared to corresponding covalently crosslinked hydrogels. These results underscore the importance of crosslinking method in maintaining hydrogel structural integrity. Although previous reports support this observation, there are other formulations of alginate that may give rise to better structural properties *in vivo*⁵⁶. Alginate is composed of (1–4)-linked β -D-manuronic acid (M) and α -L-guluronic acid (G) monomers. The relative amounts of M and G monomers vary between species of algae. During ionic crosslinking, carboxyl functional groups within the G subunits of adjacent alginate chains are ionically linked to form a semi-solid structure. As ionic crosslinking is dependent on the available G monomers, alginate polymers composed of a higher percentage of G monomers produce stiffer hydrogels and are more stable *in vivo*⁵⁷. For the purpose of this study, modified alginate was used for all hydrogels to eliminate the effect of modification on the behavior of encapsulated cells. Even though the alginate used here may not have been optimal, analyses revealed increased cellular viability and protein deposition in photo-crosslinked alginate. Moreover, the pericellular localization of ECM macromolecules in the photo-crosslinked alginate constructs was more analogous to the native tissue structure than the micro-environment observed in the ionically crosslinked alginate.

Significant increases in gene expression and ECM accumulation were measured in photo-crosslinked alginate

hydrogels at 8 weeks *in vivo*. Increased expression of type II collagen and aggrecan combined with low expression of type I collagen indicate that encapsulated cells maintained their differentiated phenotype. A significant increase in proteoglycan expression was detected between 4 and 8 weeks, while type II collagen exhibited an increasing trend that was not statistically different. Of particular interest is the increase in proteoglycan content, which has been shown to be important for functional compressive properties^{27,57}. However, compared to the GAG content of native sheep NP ($20.88 \pm 4.82 \mu\text{g}/\text{mg}$ tissue), these cell-seeded constructs only reached 3% of native levels²⁷. It is important to consider that a low cell seeding density of 10×10^6 cells/mL was used here to specifically examine the effect of the biomaterial on cellular behavior. Typically, cell-seeded hydrogel constructs for tissue regeneration use between 20×10^6 and 60×10^6 cells/mL. As such, the low initial seeding density may have contributed to the low levels of ECM production⁵⁸. It should also be noted that the modification of alginate for covalent crosslinking alters the *in vitro* and *in vivo* degradation profile of the polymer. In general, the degradation of the biomaterial scaffold may allow for increased ECM accumulation in tissue-engineered constructs^{56,59,60}. Therefore, it is possible that the improved stability of the photo-crosslinked alginate hydrogels afforded by the covalent interchain crosslinks also prevented the uniform distribution and assembly of ECM molecules from reaching native tissue levels. Although most of the materials currently under development

for intradiscal replacement are non-degradable synthetic polymers, degradable subunits may be incorporated into the alginate polymer backbone to study the effect of degradation on new matrix assembly. This approach has been used successfully for both poly(ethylene glycol) and hyaluronic acid-based photo-crosslinked hydrogels^{36,61}.

In addition to increased accumulation of characteristic ECM proteins, mechanical properties of cell-encapsulated, photo-crosslinked hydrogels exhibited significant increases over time, indicating the production of a mechanically functional matrix. At 4 weeks *in vivo*, acellular controls appeared transparent and had an equilibrium Young's modulus that was significantly lower than cell-laden hydrogels. This implies that the opacity of the constructs was due to the activity of implanted cells rather than to host cells migrating into the constructs. This also demonstrates that the increased mechanical properties were a result of cellular activity as opposed to a change in hydrogel structure. Interestingly, despite no apparent ECM accumulation, the modulus of acellular photo-crosslinked hydrogels was significantly greater than pre-implantation cell-laden constructs. This was likely due to the presence of fragments from the thin fibrous capsule that enveloped the hydrogels *in vivo*, which may have contributed to modest contraction and stiffening of the samples. After 8 weeks *in vivo*, NP cell-encapsulated, photo-crosslinked alginate hydrogels had an equilibrium Young's modulus of 4.31 ± 1.39 kPa, which is close to the native NP equilibrium modulus reported in previous studies that employed similar unconfined compression testing protocols to determine the material properties of native NP tissue (5–6.7 kPa)^{32,62,63}.

In conclusion, the results of this study support the use of photo-crosslinked alginate constructs for NP repair, as the hydrogel maintains the differentiated phenotype and allows for the assembly of functional matrix. The purpose of this investigation was to analyze the interaction between photo-crosslinked alginate and cellular behavior, particularly focusing on characteristic ECM production and function. Future studies will focus on optimizing culture conditions for NP tissue regeneration. The effect of cell seeding density, mechanical stimulation, and additional polymer chemistries may be investigated to increase the accumulation of ECM macromolecules. Furthermore, various cell sources may be used to explore the inductive potential of the photo-crosslinked alginate environment. Refinement of these parameters may lead to an injectable therapy for disc degeneration, and possibly for the repair of other cartilaginous tissues, such as hyaline articular cartilage.

Conflict of interest

None of the authors have any financial or personal relationships with any individual or organization that could inappropriately influence this work.

Acknowledgments

This work was supported by grants from the NIH (EB002425) and the Wallace H. Coulter Foundation. The authors would like to thank Dr Jason Burdick and his laboratory for assistance with experimental methods and helpful discussions and Dr Monika Damek-Poprawa for her assistance in conducting animal studies. Funding sources: National Institutes of Health and the Wallace H. Coulter Foundation.

References

- Marchand F, Ahmed AM. Investigation of the laminate structure of lumbar disc anulus fibrosus. *Spine* 1990;15:402–10.
- Antoniou J, Steffen T, Nelson F, Winterbottom N, Hollander AP, Poole RA, *et al*. The human lumbar intervertebral disc. Evidence for changes in the biosynthesis and denaturation of the extracellular matrix with growth, maturation, ageing, and degeneration. *J Clin Invest* 1996;98:996–1003.
- Bayliss MT, Johnstone B, O'Brien JP. Proteoglycan synthesis in the human intervertebral disc; variation with age, region and pathology. *Spine* 1988;13:972–81.
- Oegema TR. Biochemistry of the intervertebral disc. *Clin Sports Med* 1993;12:419–39.
- Urban JPG. The effect of physical factors on disk cell metabolism. In: Buckwalter JA, Ed. *Musculoskeletal Soft-Tissue Aging: Impact on Mobility*. Rosemont, IL: American Academy of Orthopaedic Surgeons; 1993:391–412.
- Jensen M, Kelly A, Brant-Zawadzki M. MRI of degenerative disease of the lumbar spine. *Magn Reson Q* 1994;10:173–90.
- Kestle J, Resch L, Tator C, Kucharczyk W. Intervertebral disc embolization resulting in spinal cord infarction. Case report. *J Neurosurg* 1989;71:938–41.
- Lee C. Accelerated degeneration of the segment adjacent to a lumbar fusion. *Spine* 1988;13:375–7.
- Alini M, Li W, Markovic P, Aebi M, Spiro RC, Roughley P. The potential and limitations of a cell-seeded collagen/hyaluronan scaffold to engineer an intervertebral disc-like matrix. *Spine* 2003;28:446–54.
- Sakai D, Mochida J, Yamamoto Y, Nomura T, Okuma M, Nishimura K, *et al*. Transplantation of mesenchymal stem cells embedded in Atelocollagen(F) gel to the intervertebral disc: a potential therapeutic model for disc degeneration. *Biomaterials* 2003;24:3531–41.
- Sakai D, Mochida J, Iwashina T, Hiyama A, Omi H, Imai M, *et al*. Regenerative effects of transplanting mesenchymal stem cells embedded in atelocollagen to the degenerated intervertebral disc. *Biomaterials* 2006;27:335–45.
- Sakai D, Mochida J, Iwashina T, Watanabe T, Suyama K, Ando K, *et al*. Atelocollagen for culture of human nucleus pulposus cells forming nucleus pulposus-like tissue in vitro: influence on the proliferation and proteoglycan production of HNPSV-1 cells. *Biomaterials* 2006;27:346–53.
- Gruber HE, Leslie K, Ingram J, Norton HJ, Hanley EN. Cell-based tissue engineering for the intervertebral disc: in vitro studies of human disc cell gene expression and matrix production within selected cell carriers. *Spine J* 2004;4:44–55.
- Gruber HE, Hanley EN. Human disc cells in monolayer vs 3D culture: cell shape, division and matrix formation. *BMC Musculoskelet Disord* 2000;1:1.
- Wang JY, Baer AE, Kraus VB, Setton LA. Intervertebral disc cells exhibit differences in gene expression in alginate and monolayer culture. *Spine* 2001;26:1747–51. 1752.
- Maldonado BA, Oegema TR. Initial characterization of the metabolism of intervertebral disc cells encapsulated in microspheres. *J Orthop Res* 1992;10:677–90.
- Gruber HE, Stasky AA, Hanley EN. Characterization and phenotypic stability of human disc cells in vitro. *Matrix Biol* 1997;16:285–8.
- Chiba K, Andersson GB, Masuda K, Thonar EJ. Metabolism of the extracellular matrix formed by intervertebral disc cells cultured in alginate. *Spine* 1997;22:2885–93.
- Rowley J, Mooney D. Alginate type and RGD density control myoblast phenotype. *J Biomed Mater Res* 2002;60:217–23.
- Alsberg E, Anderson KW, Albeiruti A, Rowley JA, Mooney DJ. Engineering growing tissues. *Proc Natl Acad Sci* 2002;99:12025–30.
- Drury JL, Dennis RG, Mooney DJ. The tensile properties of alginate hydrogels. *Biomaterials* 2004;25:3187–99.
- LeRoux M, Guilak F, Setton L. Compressive and shear properties of alginate gel: effects of sodium ions and alginate concentration. *J Biomed Mater Res A* 1999;47:46–53.
- Maguire T, Davidovich AE, Wallenstein EJ, Novik E, Sharma N, Pedersen H, *et al*. Control of hepatic differentiation via cellular aggregation in an alginate microenvironment. *Biotechnol Bioeng* 2007;98:631–44.
- Li X, Liu T, Song K, Yao L, Ge D, Bao C, *et al*. Culture of neural stem cells in calcium alginate beads. *Biotechnol Prog* 2006;22:1683–9.
- Kuo CK, Ma PX. Ionically crosslinked alginate hydrogels as scaffolds for tissue engineering: part 1. Structure, gelation rate and mechanical properties. *Biomaterials* 2001;22:511–21.
- Melrose J, Smith S, Ghosh P. Assessment of the cellular heterogeneity of the ovine intervertebral disc: comparison with synovial fibroblasts and articular chondrocytes. *Eur Spine J* 2003;12:57–65.
- Mizuno H, Roy A, Zaporozhan V, Vacanti C, Ueda M, Bonassar L. Biomechanical and biochemical characterization of composite tissue-engineered intervertebral discs. *Biomaterials* 2006;27:362–70.

28. Gruber HE, Fisher Jr EC, Desai B, Stasky AA, Hoelscher G, Hanley Jr EN. Human intervertebral disc cells from the annulus: three-dimensional culture in agarose or alginate and responsiveness to TGF- β 1. *Exp Cell Res* 1997;235:13–21.
29. Mizuno H, Roy A, Vacanti C, Kojima K, Ueda M, Bonassar L. Tissue-engineered composites of annulus fibrosus and nucleus pulposus for intervertebral disc replacement. *Spine* 2004;29:1290–7. discussion 1297–8.
30. Roughley P, Hoemann C, DesRosiers E, Mwale F, Antoniou J, Alini M. The potential of chitosan-based gels containing intervertebral disc cells for nucleus pulposus supplementation. *Biomaterials* 2006;27:388–96.
31. Mwale F, Iordanova M, Demers CN, Steffen T, Roughley P, Antoniou J. Biological evaluation of chitosan salts cross-linked to genipin as a cell scaffold for disk tissue engineering. *Tissue Eng* 2005;11:130–40.
32. Cloyd J, Malhotra N, Weng L, Chen W, Mauck R, Elliott D. Material properties in unconfined compression of human nucleus pulposus, injectable hyaluronic acid-based hydrogels and tissue engineering scaffolds. *Eur Spine J* 2007;16:1892–8.
33. Shao X, Hunter CJ. Developing an alginate/chitosan hybrid fiber scaffold for annulus fibrosus cells. *J Biomed Mater Res A* 2007;82A:701–10.
34. Perka C, Arnold U, Spitzer R-S, Lindenhayn K. The use of fibrin beads for tissue engineering and subsequent transplantation. *Tissue Eng* 2001;7:359–61.
35. Baer AE, Wang JY, Kraus VB, Setton LA. Collagen gene expression and mechanical properties of intervertebral disc cell-alginate cultures. *J Orthop Res* 2001;19:2–10.
36. Bryant SJ, Durand KL, Anseth KS. Manipulations in hydrogel chemistry control photoencapsulated chondrocyte behavior and their extracellular matrix production. *J Biomed Mater Res A* 2003;67A:1430–6.
37. Leach JB, Bivens KA, Patrick CW, Schmidt CE. Photocrosslinked hyaluronic acid hydrogels: natural, biodegradable tissue engineering scaffolds. *Biotechnol Bioeng* 2003;82:578–89.
38. Wang D, Williams C, Yang F, Cher N, Lee H, Elisseeff J. Bioresponsive phosphoester hydrogels for bone tissue engineering. *Tissue Eng* 2005;11:201–13.
39. Li Q, Williams CG, Sun DDN, Wang J, Leong K, Elisseeff JH. Photocrosslinkable polysaccharides based on chondroitin sulfate. *J Biomed Mater Res A* 2004;68A:28–33.
40. Anseth KS, Metters AT, Bryant SJ, Martens PJ, Elisseeff JH, Bowman CN. In situ forming degradable networks and their application in tissue engineering and drug delivery. *J Control Release* 2002;78:199–209.
41. Elisseeff J, Anseth K, Sims D, McIntosh W, Randolph M, Yaremchuk M, *et al.* Transdermal photopolymerization of poly(ethylene oxide)-based injectable hydrogels for tissue-engineered cartilage. *Plast Reconstr Surg* 1999;104:1014–22.
42. Elisseeff J, McIntosh W, Anseth K, Riley S, Ragan P, Langer R. Photoencapsulation of chondrocytes in poly(ethylene oxide)-based semi-interpenetrating networks. *J Biomed Mater Res* 2000;51:164–71.
43. Smeds K, Pfister-Serres A, Miki D, Dastgheib K, Inoue M, Hatchell D, *et al.* Photocrosslinkable polysaccharides for in situ hydrogel formation. *J Biomed Mater Res* 2001;54:115–21.
44. Burdick J, Chung C, Jia X, Randolph M, Langer R. Controlled degradation and mechanical behavior of photopolymerized hyaluronic acid networks. *Biomacromolecules* 2005;6:386–91.
45. Bryant S, Nuttelman C, Anseth K. Cytocompatibility of UV and visible light photoinitiating systems on cultured NIH/3T3 fibroblasts in vitro. *J Biomater Sci Polym Ed* 2000;11:439–57.
46. Nettles D, Vail T, Morgan M, Grinstaff M, Setton L. Photocrosslinkable hyaluronan as a scaffold for articular cartilage repair. *Ann Biomed Eng* 2004;32:391–7.
47. Chung C, Mesa J, Miller G, Randolph M, Gill T, Burdick J. Effects of articular chondrocyte expansion on neocartilage formation in photocrosslinked hyaluronic acid networks. *Tissue Eng* 2006;12:2665–73.
48. Chou A, Reza A, Nicoll S. Distinct intervertebral disc cell populations adopt similar phenotypes in three-dimensional culture. *Tissue Eng Part A* 2008;14:2079–87.
49. Chou A, Bansal A, Miller G, Nicoll S. The effect of serial monolayer passaging on the collagen expression profile of outer and inner annulus fibrosus cells. *Spine* 2006;31:1875–81.
50. Chou A, Nicoll S. Characterization of photocrosslinked alginate hydrogels for nucleus pulposus cell encapsulation. *J Biomed Mater Res A* (In press) doi:10.1002/jbm.a.32191.
51. Wong M, Siegrist M, Goodwin K. Cyclic tensile strain and cyclic hydrostatic pressure differentially regulate expression of hypertrophic markers in primary chondrocytes. *Bone* 2003;33:685–93.
52. Reza A, Nicoll S. Hydrostatic pressure differentially regulates outer and inner annulus fibrosus cell matrix production in 3D scaffolds. *Ann Biomed Eng* 2008;36:204–13.
53. Farndale R, Sayers C, Barrett A. A direct spectrophotometric microassay for sulfated glycosaminoglycans in cartilage cultures. *Connect Tissue Res* 1982;9:247–8.
54. Enohakhare BO, Bader DL, Lee DA. Quantification of sulfated glycosaminoglycans in chondrocyte/alginate cultures, by use of 1,9-dimethylmethylene blue. *Anal Biochem* 1996;243:189–91.
55. Soltz M, Ateshian G. Experimental verification and theoretical prediction of cartilage interstitial fluid pressurization at an impermeable contact interface in confined compression. *J Biomech Eng* 1998;31:927–34.
56. Kong HJ, Alsberg E, Kaigler D, Lee KY, Mooney DJ. Controlling degradation of hydrogels via the size of crosslinked junctions. *Adv Mater* 2004;16:1917–21.
57. Roughley PJ, Alini M, Antoniou J. The role of proteoglycans in aging, degeneration and repair of the intervertebral disc. *Biochem Soc Trans* 2002;30:869–74.
58. Mauck RL, Wang CC-B, Oswald ES, Ateshian GA, Hung CT. The role of cell seeding density and nutrient supply for articular cartilage tissue engineering with deformational loading. *Osteoarthritis Cartilage* 2003;11:879–90.
59. Davis KA, Burdick JA, Anseth KS. Photoinitiated crosslinked degradable copolymer networks for tissue engineering applications. *Biomaterials* 2003;24:2485–95.
60. Augst AD, Kong HJ, Mooney DJ. Alginate hydrogels as biomaterials. *Macromol Biosci* 2006;6:623–33.
61. Sahoo S, Chung C, Khetan S, Burdick JA. Hydrolytically degradable hyaluronic acid hydrogels with controlled temporal structures. *Biomacromolecules* 2008;9:1088–92.
62. Umehara SMD, Tadano SP, Abumi KMD, Katagiri KMS, Kaneda KMD, Ukai TP. Effects of degeneration on the elastic modulus distribution in the lumbar intervertebral disc. *Spine* 1996;21:811–9.
63. Johannessen W, Vresilovic EJ, Seguritan J, Elliott D. Altered nucleus pulposus mechanics using chondroitinase-ABC and genipin as a model of early disc degeneration. *Trans Orthop Res Soc* 2004;29:1150.